



# Monte Carlo simulation of reflection effects of multi-element materials on gamma rays

Ying-Hong Zuo<sup>1</sup> · Jin-Hui Zhu<sup>1</sup> · Peng Shang<sup>1</sup>

Received: 24 August 2020 / Revised: 7 November 2020 / Accepted: 21 November 2020 / Published online: 20 January 2021  
© China Science Publishing & Media Ltd. (Science Press), Shanghai Institute of Applied Physics, the Chinese Academy of Sciences, Chinese Nuclear Society 2021

**Abstract** To study the effects of the gamma reflection of multi-element materials, gamma ray transport models of single-element materials, such as iron and lead, and multi-element materials, such as polyethylene and ordinary concrete, were established in this study. Relationships among the albedo factors of the gamma photons and energies and average energy of the reflected gamma rays by material type, material thickness, incident gamma energy, and incidence angle of gamma rays were obtained by Monte Carlo simulation. The results show that the albedo factors of single-element and multi-element materials increase rapidly with an increase in the material thickness. When the thickness of the material increases to a certain value, the albedo factors do not increase further but rather tend to the saturation value. The saturation values for the albedo factors of the gamma photons, and energies and the reflection thickness are related not only to the type of material but also to the incident gamma energy and incidence angle of the gamma rays. At a given incident gamma energy, which is between 0.2 and 2.5 MeV, the smaller the effective atomic number of the multi-element material is, the higher the saturation values of the albedo factors are. The larger the incidence angle of the gamma ray is, the greater the saturation value of the gamma albedo factor,

saturation reflection thickness, and average saturation energy of the reflected gamma photons are.

**Keywords** Multi-element materials · Gamma albedo factor · Effective atomic number · Monte Carlo simulation

## 1 Introduction

Gamma rays are uncharged streams of photons. When they interact with matter, the photons are either absorbed or scattered by the matter. The scattering of gamma photons backward from the surface of a material is referred to as backscattering (or reflection) of gamma rays. Reflection is not just defined as the reflection from the surface of a material, but rather as a complete process of radiation transmission into the target material, i.e., scattering and absorption in the material. Understanding the physical process of gamma ray transmission and reflection in the matter is of fundamental importance in gamma ray shielding, calculation of gamma radiation dose, gamma detector design, and the nondestructive testing of materials via gamma rays [1–3]. The process of gamma ray reflection in a material is closely related to the energy of the incident gamma photon, incidence angle, thickness, and elemental composition of the material. The reflection coefficient (albedo factor) of gamma rays incident on one side of the slab material can be defined as the ratio of the amount of radiation reflected from the material to the amount of radiation incident on the material. Reflection effects are formed from the multiple scattering and absorption interaction between gamma photons and the material within a certain thickness and backscattering from the surface of the material. The gamma ray albedo factor includes the

---

This work was supported by the State Key Lab of Intense Pulsed Radiation Simulation and Effect Basic Research Foundation (No. SKLIPR1504).

---

✉ Ying-Hong Zuo  
zuoyinghong@nint.ac.cn

<sup>1</sup> Northwest Institute of Nuclear Technology, Xi'an 710024, China

number albedo factor, energy albedo factor, and dose albedo factor. The number albedo factor refers to the ratio of the number of reflected gamma photons to the number of incident gamma photons. The energy albedo factor is the ratio of the total energy of the reflected gamma photons to the total energy of the incident gamma photons. The dose albedo factor can be calculated from the number albedo factor and energy albedo factor.

By means of experiments and numerical simulations, particularly through various experimental measurements, many studies have performed research on the gamma albedo of different materials. Demet et al. experimentally studied the reflection effect of 10 elements (Fe, Co, Ni, Cu, Zr, Mo, Ag, Dy, Yb, and Au) with atomic numbers ranging from 26 to 79 for a photon with energy of 59.54 keV using an HPGe detector. They obtained a third-order polynomial function relating the albedo factor and the atomic number and observed that albedo factors decreased with an increasing atomic number [1]. Uzunoglu studied the saturation thickness using gamma photons scattered from mercury(II) oxide and lead(II) oxide targets, and gamma albedo factors (albedo number, albedo energy, and albedo dose) were determined experimentally [4]. Sabharwal et al. studied the multiple scattering process and reflection effects of some single-element materials, including C, Al, Fe, Zn, and Sn, on 279 keV, 320 keV, 511 keV, 662 keV, and 1.12 MeV gamma rays. The results show that the gamma number and energy albedo factors decrease with an increase in the atomic number of the target materials [5, 6]. Diop calculated the angle and energy differential albedo factors of a half-infinite plate of iron material for 0.5, 1, 3, and 8 MeV gamma rays using the Monte Carlo program Tripoli [7]. Shimizu studied the energy and angle differential albedo factors of semi-infinite water, concrete, soil, and other media using the invariant embedding method [8]. Biswas measured the gamma ray albedo factors of tin and lead; the gamma number albedo values for Sn were obtained with 145 keV ( $^{141}\text{Ce}$ ), 279 keV ( $^{203}\text{Hg}$ ), 662 keV ( $^{137}\text{Cs}$ ), and 1250 keV ( $^{60}\text{Co}$ ) photons and for the lead with 662 keV and 1250 keV photons [9]. Seda et al. calculated the number albedo factor and energy albedo factor of 60 and 1250 keV gamma rays using the Monte Carlo method [10]. Bulatov studied the albedo factors of carbon, aluminum, iron, and lead with the gamma rays produced by  $^{60}\text{Co}$ ,  $^{137}\text{Cs}$ , and  $^{51}\text{Cr}$  sources [11].

The above-mentioned studies mainly focus on the gamma ray albedo factor of a single element (e.g., Fe, Co, Ni, Cu, Zr, Al, Zn, and Sn) with some specific gamma ray energies; however, studies on the gamma albedo factor of multi-element materials are few. In practical engineering applications, some materials are not composed of a single element but rather are composed of multiple elements. In this study, the Monte Carlo simulation method is used to

compare the gamma reflection effect for single-element and multi-element materials with a series of gamma ray energies. The effective atomic number, which is determined by considering the weights of the different partial radiation interaction processes in different energy regions, is a key parameter that can be used to characterize the radiation response of the materials and provide information as to how gamma rays interact with different types of materials, particularly multi-element materials [12–14]. The relationships between the gamma albedo factor and the effective atomic number of single-element and multi-element materials are established based on the simulation results. The influence of the shielding material thickness, energy of the incident gamma ray, and incident angle on the gamma ray albedo factors are investigated. In Sect. 2, we describe the materials and methods. The results and discussion are presented in Sect. 3, and the conclusions are presented in Sect. 4.

## 2 Materials and methods

To compare the gamma albedo factor of multi-element materials with that of single-element materials, we selected materials of both single-element and multi-element varieties and established a computational physical model consisting of a gamma ray source and shielding material body, as shown in Fig. 1. The monoenergetic gamma ray source was placed at a distance of  $l = 5$  cm from the shielding material body, which is a circular slab, and the shielding material body is irradiated vertically by gamma rays. The thickness of the circular slab material body is  $d$ , which resides within a certain range. The thickness of the material with high mass density is relatively small, whereas that of the material with low mass density is relatively larger. The radius of the circular slab shielding material is  $R = 3.5$  m, such that gamma rays cannot penetrate the round side of the shielding material. The material is

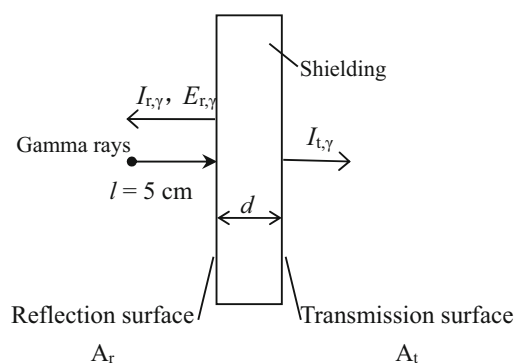


**Fig. 1** Schematic diagram of calculation physical model

surrounded by a vacuum; thus, the influence of the surrounding air on physical laws can be avoided.

The material is composed of single elements or multi-elements with different thicknesses. The materials include iron, lead, polyethylene (PE), and ordinary concrete (OC). The mass densities of the materials are 7.9, 11.35, 0.9, and 2.3 g/cm<sup>3</sup>, respectively. To describe the reflection and transmission of gamma rays more conveniently, we specified the reflection and transmission surfaces. The side of the shielding material body closer to the gamma ray source is the reflecting surface (denoted as A<sub>r</sub>) and the other side is the transmission surface (denoted as A<sub>t</sub>).

The simulation of the transport process of gamma rays in shielding materials was carried out by SuperMC 3.4.0, and the data library used in the simulation was ENDF/B-VII.1. The SuperMC program is a general, intelligent, accurate, and precise simulation software system used for nuclear design and safety evaluation of nuclear systems, which has been verified and validated by more than 2000 benchmark models and experiments [15–17]. The program can simulate the joint transport of neutrons and photons and has a strong geometric processing ability. The number of gamma rays emitted is N<sub>0</sub>, and the number of gamma rays reflected (or backscattered) by the shielding material from the reflecting surface is recorded as N<sub>r</sub> by the F1 surface flow counter card; thus, the gamma number albedo factor can be calculated as I<sub>r,γ</sub> = N<sub>r</sub>/N<sub>0</sub>. Meanwhile, the total energy E<sub>tot,r</sub> of the reflected gamma ray is recorded. Dividing the total reflected gamma energy by the total incident gamma energy yields the gamma energy albedo factor I<sub>r,E</sub>. During the calculation, if the number of gamma rays on the transmission surface is recorded as N<sub>t</sub>, the gamma transmission coefficient can be presented as I<sub>t,γ</sub> = N<sub>t</sub>/N<sub>0</sub>. The number of gamma photons in each transport simulation is 1 × 10<sup>8</sup>, which ensures that the relative error of the simulation results is less than 5%. This shows that the calculated results are credible. The calculation expressions for the gamma number albedo factor I<sub>r,γ</sub>, gamma energy albedo factor I<sub>r,E</sub>, and gamma transmission coefficient I<sub>t,γ</sub> are as follows:

$$I_{r,\gamma} = \frac{1}{N_0} \int_{A_r} dA \int_{\Omega \cdot n > 0} d\Omega \int_t dt \int_E \Psi(r, E, t, \Omega) dE, \tag{1}$$

$$I_{r,E} = \frac{1}{N_0 E_{\gamma,0}} \int_{A_r} dA \int_{\Omega \cdot n > 0} d\Omega \int_t dt \int_E E \Psi(r, E, t, \Omega) dE, \tag{2}$$

$$I_{t,\gamma} = \frac{1}{N_0} \int_{A_t} dA \int_{\Omega \cdot n > 0} d\Omega \int_t dt \int_E \Psi(r, E, t, \Omega) dE, \tag{3}$$

where  $\Psi(r, E, t, \Omega)$  represents the angular flux of gamma rays with energy  $E$  in unit energy interval of unit volume at

time  $t$  and position  $\mathbf{r}$  within a unit solid angle of direction  $\mathbf{\Omega}$  in unit time;  $\mathbf{n}$  is the external normal vector of the reflection or transmission surface;  $\mathbf{\Omega} \cdot \mathbf{n} > 0$  represents the gamma photon flow integration on the transmission surface; and  $E_{\gamma,0}$  is the energy of the incident gamma ray.

For multi-element materials, the mass attenuation coefficient can be obtained by the weighted summation of the mass attenuation coefficients for each element. The theoretical expression of the mass attenuation coefficient of multi-element materials is [18–20]

$$\frac{\mu}{\rho} = \sum_i w_i \left(\frac{\mu}{\rho}\right)_i \tag{4}$$

Here,  $w_i$  and  $\rho_i$  are the mass percent of the  $i$ th element and mass attenuation coefficient of gamma rays in a molecule, respectively. The mass percentage is calculated by the following relation:

$$w_i = \frac{n_i A_i}{\sum_i n_i A_i}, \tag{5}$$

where  $A_i$  is the atomic weight of the  $i$ th element and  $N_i$  is the atomic number of the  $i$ th element in a molecule. According to the mass attenuation coefficient  $\mu/\rho$ , the total atomic cross section  $\sigma_{t,a}$  and total electronic cross section  $\sigma_{t,e}$  can be calculated as [21]

$$\sigma_{t,a} = \frac{1}{N_A} \sum_i f_i A_i \left(\frac{\mu}{\rho}\right)_i, \tag{6}$$

$$\sigma_{t,e} = \frac{1}{N_A} \sum_i \frac{f_i A_i}{Z_i} \left(\frac{\mu}{\rho}\right)_i, \tag{7}$$

where  $f_i$  is the atomic number percentage of the  $i$ th element in the substance,  $Z_i$  is the atomic number of the  $i$ th element, and  $N_A$  is Avogadro’s number. With  $\sigma_{t,a}$  and  $\sigma_{t,e}$ , the effective atomic number  $Z_{\text{eff}}$  of the multi-element composition can be calculated by the ratio of  $\sigma_{t,a}$  to  $\sigma_{t,e}$ :

$$Z_{\text{eff}} = \frac{\sigma_{t,a}}{\sigma_{t,e}} \tag{8}$$

The effective atomic number  $Z_{\text{eff}}$  is a key parameter that can provide information on how gamma rays interact with different types of materials, especially multi-element materials;  $Z_{\text{eff}}$  can represent the effective charge number of the multi-component materials. From the calculation expressions, the effective atomic number is related not only to the energy of the gamma ray but also to the elemental composition of the material. In the next section, the relationship between the gamma albedo factor and the effective atomic number for multi-element materials for gamma rays of various energies is discussed.

### 3 Results and discussion

There are three main types of interactions between gamma rays and matter: photoelectric effect, Compton scattering, and electron pair production. The type of interaction depends on the energy of the gamma rays and the types of elements that interact with the photon. The detailed photon transport simulation process is adopted by default in our simulations using SuperMC. This means that photon transport includes the photoelectrical effect, coherent scattering, Compton scattering, and electron pair production. The results of the number albedo measurement of 0.662 keV gamma rays from a 3.5-cm-thick iron circular slab are provided in Ref. [22] and its citations. We established a Monte Carlo calculation model that considers the same layout as the experimental geometric layout in Ref. [22]. The gamma number albedo of the iron circular slab in the same model in Ref. [22] is calculated to be 0.321, which is consistent with the experimental results of  $0.35 \pm 0.01$  and 0.32 provided in Ref. [22] and its citations.

According to the computational physical model described in Sect. 2, the Monte Carlo method is used to simulate the interaction process of gamma rays with different energies incident on single-element or multi-element materials with different thicknesses. The relationship among the gamma number albedo factor, gamma energy albedo factor and material type, material thickness, incident gamma energy, incident angle, and other relative parameters is obtained.

#### 3.1 Effect of material thickness on the gamma albedo factor

Figure 2a–d shows the curves of the gamma transmission coefficient and gamma number albedo factor with respect to material thickness when the monoenergetic energy gamma ray is vertically incident on iron, lead, PE, and OC materials. Figure 2a and b shows that the transmission coefficient of gamma rays decreases exponentially with an increase in the shielding material thickness. At a certain thickness, the higher mass density of the material corresponds to a lower gamma ray transmission coefficient, which is consistent with the calculation results of previous studies [23]. However, the variation curve of the gamma number albedo factor with respect to the material thickness shown in Fig. 2c and d is different from that of the transmission coefficient with respect to material thickness. For both single-element and multi-element materials, the gamma number albedo factor increases rapidly with increasing material thickness; however, as the thickness

reaches a certain value, the albedo factor does not continue to increase but rather tends to saturation.

When the material is thin, the gamma ray easily penetrates the material, causing a weak reflection effect. With an increase in the thickness of the shielding material, especially when the thickness reaches more than twice the mean free path of the incident gamma ray, gamma rays are scattered multiple times in the material. The number of multiple backscattered events increases, wherein more gamma rays are scattered or absorbed by the material. In addition, the number of gamma photons that can penetrate the material is also reduced to a certain extent, enhancing the reflection effect. When the thickness of the material reaches a certain value, the multiple scattering or absorption of gamma rays by the material reaches an equilibrium; this condition is considered to be saturation of the gamma albedo factor. A comparison of the simulation results of single-element materials—iron and lead—shows that the smaller the atomic number of the single-element material is, the higher the gamma albedo factor is; as the thickness of the corresponding material increases, the gamma ray albedo factor approaches saturation. This conclusion is consistent with the results that the numbers of gamma photon multiple backscattered events show an increase with increasing target thickness and then saturate for a particular thickness of the target in References [5, 6], verifying the correctness of the simulation results of this study.

For gamma rays with energies of 0.662 or 1.25 MeV, using the elemental compositions of PE (atomic number percentages of H and C are 0.3333 and 0.6667, respectively) and OC (atomic number percentages of H, C, O, Na, Mg, Al, Si, K, Ca, and Fe are 0.3042, 0.0029, 0.496, 0.0092, 0.0007, 0.0103, 0.1505, 0.0071, 0.0149, and 0.0016, respectively), the effective atomic numbers of PE are calculated as 2.528 and 2.676 and those of OC are 9.159 and 7.151. The simulation results of the multi-element materials (Fig. 2c and d) show that when the energy of the incident gamma ray is 0.662 and 1.25 MeV, respectively, a smaller effective atomic number of the material corresponds to a higher gamma number albedo factor when the reflection effect reaches saturation and the material thickness is large. For example, for gamma rays with an energy of 1.25 MeV, when the reflections for PE, OC, iron, and lead reach saturation, the gamma number albedo factor and the saturation reflection thickness of the material decreases, and the corresponding effective atomic number relationship is  $2.676 < 7.151 < 26 < 82$ .

Figure 2c and d shows that for single-element and multi-element materials, when the thickness of the material is small (i.e., material thickness is less than approximately 0.08 cm and the thickness is significantly different from the saturation reflection thickness), the gamma ray number

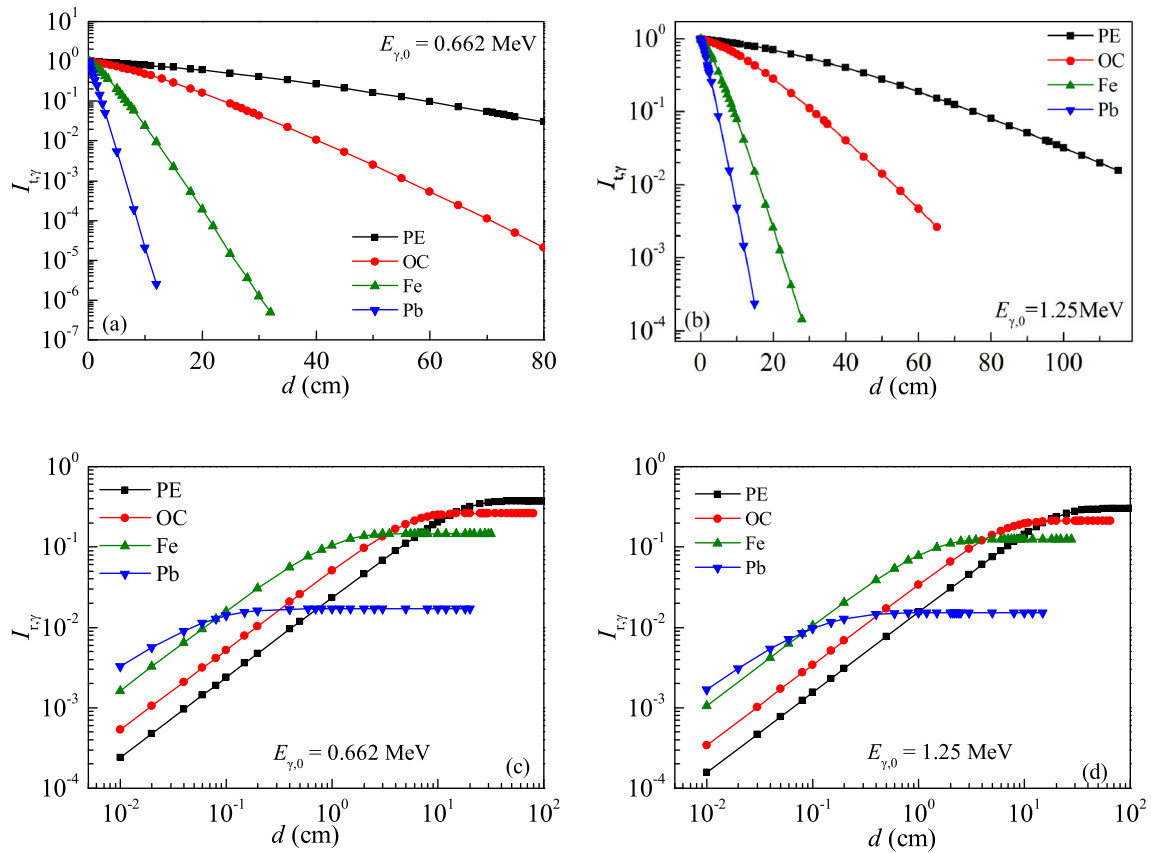


**Fig. 2** (Color online) Transmission coefficient and gamma number albedo factor versus material thickness. **a** Transmission coefficient for 0.662 MeV gamma; **b** Transmission coefficient for 1.25 MeV

gamma; **c** Number albedo factor for 0.662 MeV gamma; **d** Number albedo factor for 1.25 MeV gamma

albedo factors of PE, OC, iron, and lead increase under the same thickness condition, whether the gamma energy is 0.662 or 1.25 MeV. When the material is thin, i.e., the thickness of the material is far from the saturation reflection thickness; higher elemental atomic numbers correspond to stronger interactions between the gamma ray and the material, resulting in higher gamma ray albedo factors.

Figure 3 shows the variation curve of the gamma energy albedo factor with material thickness. As shown in Fig. 3, for single-element or multi-element materials, when the incident gamma energy is 0.662 or 1.25 MeV, the energy albedo factor of the gamma ray first increases and then tends to saturation with an increase in the material thickness. This is similar to the behavior of the gamma number albedo factor with material thickness. A comparison of the

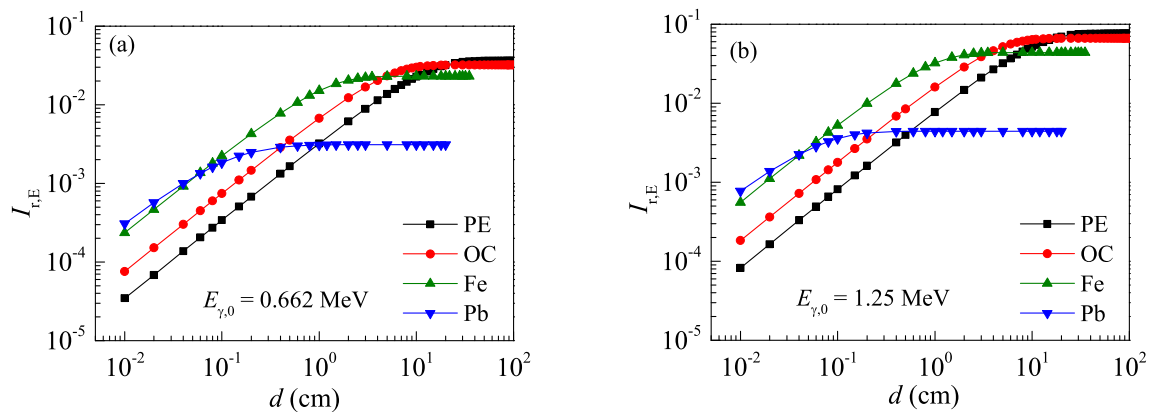


**Fig. 3** (Color online) Gamma energy albedo factor versus material thickness. **a** For 0.662 MeV gamma ray; **b** For 1.25 MeV gamma ray

gamma ray energy albedo factor of single-element material iron and lead and multi-element material PE and OC shows that the larger the effective atomic number of the material is, the smaller the gamma energy albedo factor is when the reflection effect reaches saturation as the corresponding material thickness is smaller. For example, for a gamma ray of energy 0.662 MeV, when the reflection for PE, OC, iron, and lead reaches saturation, the gamma energy albedo factor decreases and the saturation gamma energy albedo factors yield the values of 0.0361, 0.0320, 0.0230, and 0.0003, respectively. In addition, the saturation reflection thickness of the material decreases, showing the values of 60, 28, 6.5, and 0.6 cm, and the corresponding effective atomic number relationship is 2.676, 7.151, 26, and 82.

For the convenience of research, we provide the following definition: when the change rate  $\delta_\gamma$  of the gamma albedo factor with an increase in the material thickness is less than 0.01%, the corresponding thickness is defined as the saturation gamma reflection thickness and the albedo factor is called the saturation gamma albedo factor. According to the definition, the change rate  $\delta_\gamma$  is calculated as

$$\delta_\gamma = \frac{I_r(d_2) - I_r(d_1)}{d_2 - d_1}, \tag{9}$$

where  $I_r(d_1)$  and  $I_r(d_2)$  are the gamma albedo factors corresponding to the shielding material thickness  $d_1$  and  $d_2$ , respectively, and  $d_2 > d_1$ . According to the previous simulation results, the gamma albedo factor tends to saturate with an increase in the material thickness; thus,  $\delta_\gamma$  gradually tends to zero with an increase in the material thickness.

According to the above definition, the saturation gamma number albedo factor  $I_{r,\gamma,st}$ , saturation gamma reflection thickness  $d_{r,st}$ , and saturation gamma energy albedo factor  $I_{r,E,st}$  of four typical shielding materials were calculated, as shown in Table 1. Table 1 shows that for gamma rays with energies of 0.662 and 1.25 MeV, when the incident gamma energy is constant, the effective atomic number  $Z_{eff}$  of PE, OC, iron, and lead gradually increases, causing the saturation gamma number albedo factor and saturation gamma

energy albedo factor to decrease in turn. For gamma rays with an energy of 1.25 MeV, the saturation reflection thickness of the PE material (75 cm) and the corresponding saturation gamma number albedo factor are the largest (29.7%). Meanwhile, the saturation reflection thickness of lead is the smallest, at 1.5 cm, and the corresponding saturation gamma number albedo factor is also at a minimum, 1.53%. The saturation reflection thickness and saturation albedo factor are related to not only the material type but also the incident gamma energy. For low incident energy, the penetration of gamma photons into certain materials is low; hence, the probability of backscattered gamma photons coming out from the reflection surface is enhanced. The lower the gamma photon energy is, the smaller the fractional energy loss of a photon per collision is. Thus, the amount of energy carried by the reflected gamma photon becomes a larger fraction of the incident energy.

### 3.2 Influence of incident gamma energy on gamma albedo factor

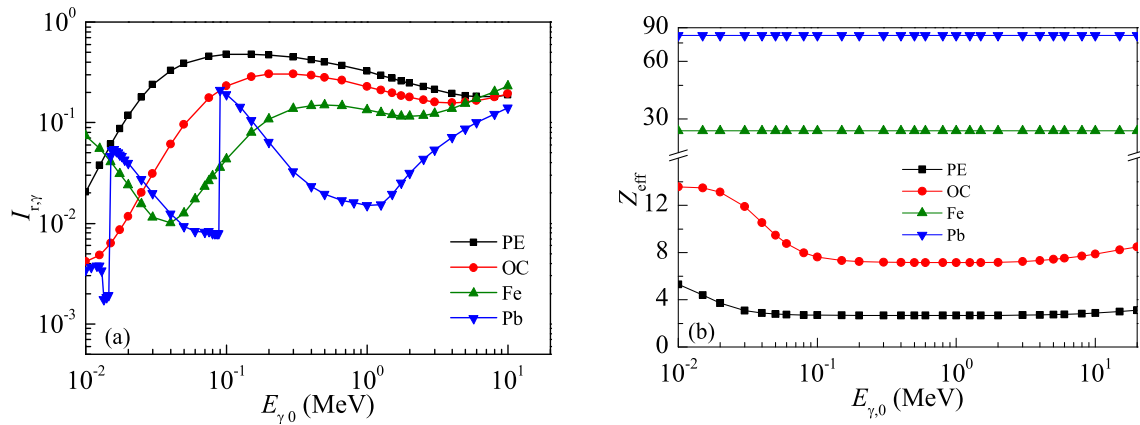
To analyze the influence of incident gamma energy on the saturation gamma albedo factor, the thickness of the material in the calculation model is set to be larger than the saturation reflection thickness; the variation of the saturation gamma albedo factor with the incident gamma energy is calculated using a Monte Carlo simulation. The incident gamma photons come out from the reflection surface with reduced energy, the value of which depends on the scattering angle. By analyzing the influence of the incident gamma energy on the albedo factor, the dependence of gamma ray reflection or backscattering on the photon energy is discussed in this section.

Figure 4 shows the variation of the saturation gamma albedo factor with incident gamma energy for iron, lead, PE, and OC thicknesses of 20, 10, 110, and 50 cm, respectively. In Ref. [8], the saturation reflection coefficients of lead, OC, and iron for 1 MeV gamma rays were calculated as 0.0151, 0.217, and 0.134, respectively, using the MCNP4A program and the invariant embedding method. In this study, the saturation reflection coefficients of lead, OC, and iron for 1 MeV gamma rays are calculated as 0.0150, 0.229, and 0.134, respectively, by SuperMC simulation, as shown in Fig. 4. The simulation results in this study are basically consistent with those in Ref. [8], except that those for concrete materials are slightly different owing to the influence of component differences, which further verifies the correctness of the simulation results in this study.

Figure 4 shows that for PE and OC, when the thickness exceeds the saturation gamma reflection thickness, with the incident gamma energy gradually increasing from 0.01 to 10 MeV, the saturation gamma reflection first increases

**Table 1** Saturation gamma albedo factor, saturation gamma energy albedo factor, and saturation gamma reflection thickness

Material	$E_{\gamma,0} = 0.662 \text{ MeV}$			$E_{\gamma,0} = 1.25 \text{ MeV}$		
	$d_{r,st} \text{ (cm)}$	$I_{r,\gamma,st}$	$I_{r,E,st}$	$d_{r,st} \text{ (cm)}$	$I_{r,\gamma,st}$	$I_{r,E,st}$
PE	60	0.3690	0.0361	75	0.2969	0.0761
OC	28	0.2623	0.0320	34	0.2110	0.0661
Iron	6.5	0.1468	0.0230	7.5	0.1252	0.0438
Lead	0.6	0.0169	0.0003	1.5	0.0153	0.0044



**Fig. 4** (Color online) Influence of incident gamma energy. **a** Saturation gamma number albedo factor; **b** Effective atomic number of material

and then decreases. When the gamma ray energy is between 0.01 and 5 MeV, the gamma number albedo of PE material is higher than that of OC material under the same material thickness. The saturation gamma albedo factor of PE for gamma rays of energy 0.15 MeV is the highest, which is approximately 47.9%, and that of OC for gamma rays of energy 0.3 MeV is the highest, which is approximately 30.4%. For single-element material, the saturation gamma albedo factor decreases first and then increases with an increase in the incident gamma energy; the saturation gamma albedo factor of the iron material for 0.04 MeV gamma is the smallest, which is approximately 1.0%. For single-element material lead, the saturation gamma albedo factor changes twice with an increase in the incident gamma energy, with corresponding gamma ray energies of 0.015 and 0.09 MeV, respectively. This is mainly because there is a jump in the mass attenuation coefficient of lead for gamma rays near the two energies.

The curve of the effective atomic number versus gamma energy in Fig. 4b reveals that when the gamma ray energy is between 0.01 and 0.1 MeV, the effective atomic number of PE and OC materials decreases with an increase in the gamma ray energy. When the energy of the gamma ray is higher than 0.1 MeV, the effective atomic number of PE and concrete remains approximately unchanged with an increase in gamma ray energy. When the gamma ray energy is between 0.01 and 10 MeV, the effective atomic number of PE is greater than that of OC. When the incident gamma energy is between 0.2 MeV and 5 MeV, the saturation gamma number albedo factors of single-element materials iron and lead and multi-element materials PE and OC increase with a decrease in the effective atomic number; i.e., the saturation gamma number albedo factors of lead, iron, OC, and PE increase.

Figure 5 shows the relationship between the saturation gamma energy albedo factor and saturation average energy of gamma reflection with respect to the incident gamma

energy. Figure 5a shows that the variation in the saturation gamma energy albedo factor with incident gamma energy is similar to that of the saturation gamma number albedo factor. When the incident gamma energy is between 0.2 and 2.5 MeV, the saturation gamma energy albedo factors of lead, iron, OC, and PE increase with a decrease in the effective atomic number. The dependence of the albedos on the effective atomic number can be explained by the increase in the Compton scattering cross section with an increase in the atomic number of the target material.

The results in Ref. [24] show that the number of multiple backscattered events increases with increasing target thickness, saturating for a particular target thickness. The Monte Carlo calculation results in Ref. [24] also support the present results. Figure 5b indicates that the variation in the average energy of the saturation reflection gamma rays of PE, OC, iron, and lead with incident gamma energy is more complex than the gamma number and gamma energy albedo factors. For different incident gamma energies, there is no consistent change rule for the average energy of the saturation reflection gamma rays. In general, the average energy of the saturation of the reflected gamma increases with an increase in the incident gamma energy. In different energy regions, the relative values of the average energy of the saturation of the reflected gamma rays of the materials are different. When the incident gamma ray energy is between 1.25 and 10 MeV and remains constant, the average energies of the saturation of the reflected gamma rays of PE, OC, iron, and lead increase.

### 3.3 Influence of gamma incidence angle on albedo factor

Differential albedo has been addressed in many studies [1, 6, 9]. In this study, the integral albedo, i.e., the integration of all gamma rays scattered from different directions on the surfaces of the shielding materials, is the focus;

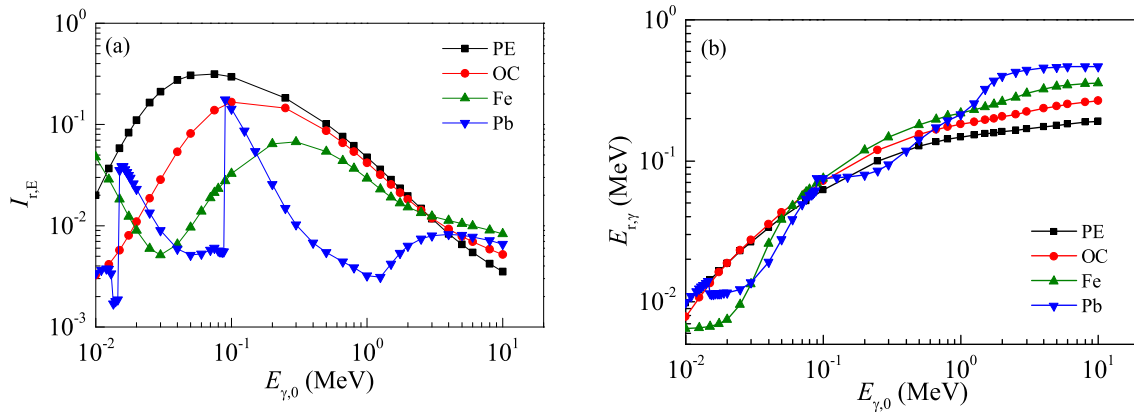


**Fig. 5** (Color online) Influence of incident gamma energy. **a** Saturation gamma energy albedo factor; **b** Average energy of saturation of the reflected gamma rays

likewise, the influence of different incident angles on the integral albedo is highlighted. The multiple scattering processes of gamma rays in shielding materials and scattering in different directions have been considered in the simulation process using the Monte Carlo method. Figure 6 shows the variation in the gamma number albedo factor and average energy of the reflection gamma with the thickness of single-element material iron at different incident angles with a gamma ray energy of 1.25 MeV, where  $\theta$  is the angle between the incident direction of the gamma ray and the normal direction of the iron surface.

When the gamma ray is obliquely incident onto the material, for a certain material thickness, larger incident angles correspond to interactions at larger distances between the gamma ray and the material as the ray penetrates the material. Figure 6 shows the saturation reflection thickness and saturation gamma albedo factor in the case of oblique gamma ray incidence. The larger the angle is between the incident direction of the gamma ray and the normal direction of the material surface, the greater the thickness of the saturation reflection, saturation gamma

number albedo factor, and average energy of the saturation gamma reflection are. The larger the angle of oblique incidence of gamma rays is, the more the gamma rays that leave the material, owing to scattering over a long distance in the direction of the oblique gamma ray path within the same depth range close to the surface of the material. This corresponds to a greater gamma number albedo factor. Figure 6b shows that the average energy of the reflected gamma rays of iron first decreases with an increase in the material thickness and then tends to a saturation value when the incident angle and incident gamma energy are fixed. The larger the angle of oblique incidence is, the greater the saturation value of the average energy of the reflected gamma rays is. For incident gamma rays of 1.25 MeV at an iron thickness of greater than 10 cm, the saturation values of the average energy of the reflected gamma rays are 0.230, 0.234, 0.248, 0.275, and 0.321 for incident angles of  $0^\circ$ ,  $15^\circ$ ,  $30^\circ$ ,  $45^\circ$ , and  $60^\circ$ , respectively.

Figure 7a–d shows the variation curves of saturation gamma number albedo factor and average energy of the saturation of the reflected gamma rays of iron at a thickness

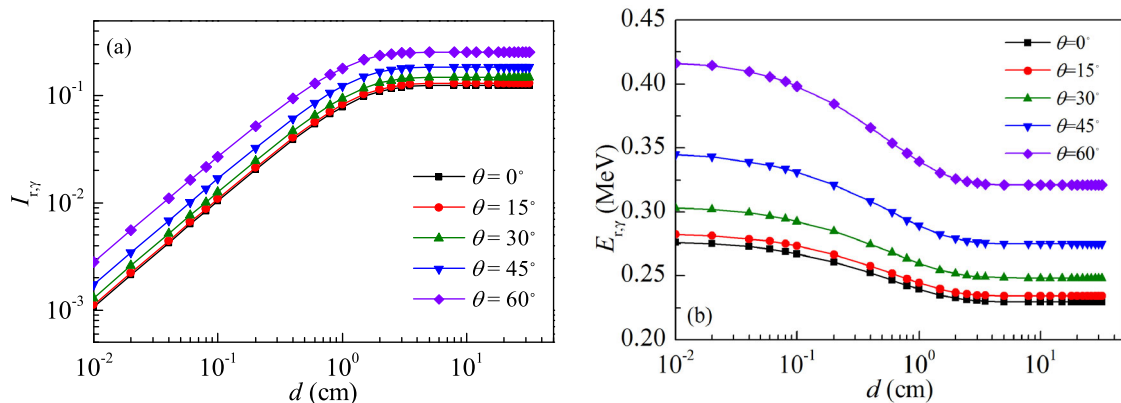


**Fig. 6** (Color online) Results for different gamma ray incidence angles. **a** Gamma number albedo factor versus material thickness; **b** Average energy of the reflected gamma rays versus material thickness

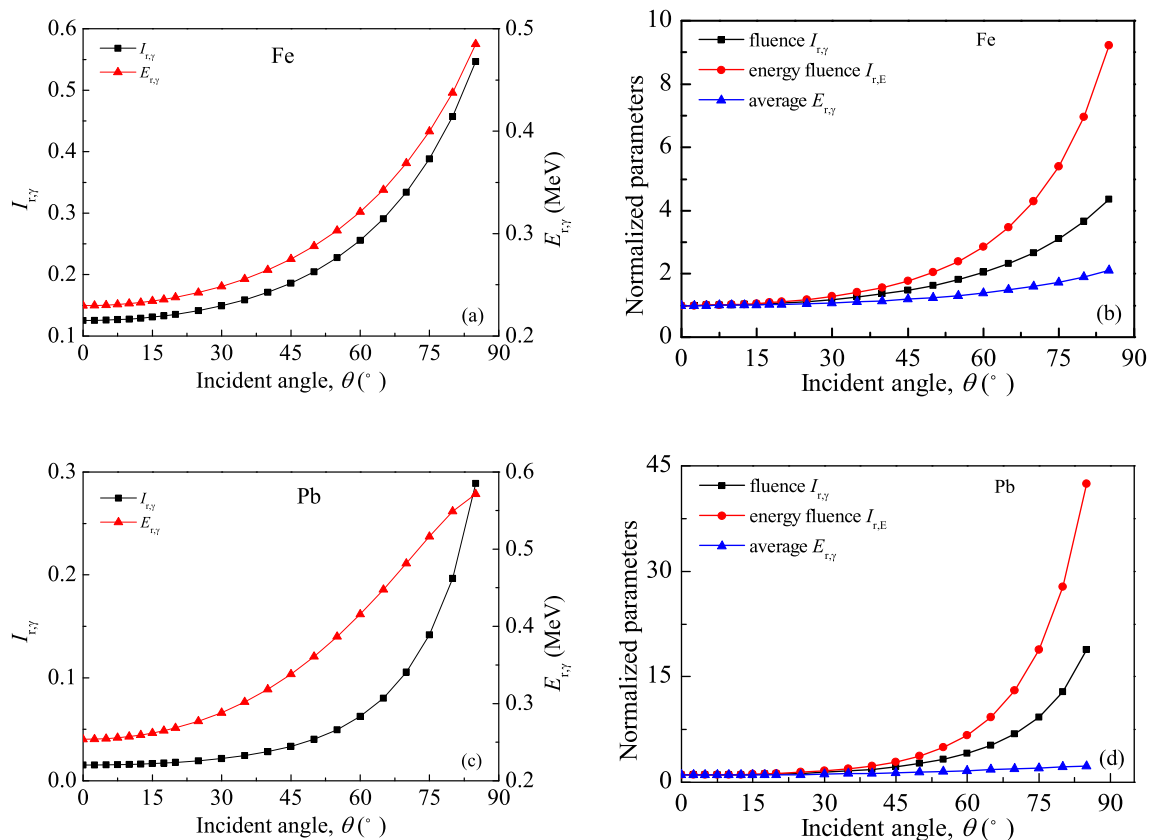


**Fig. 7** (Color online) Results of iron with a thickness of 28 cm and lead with a thickness of 10 cm for 1.25 MeV gamma. **a** Saturated gamma number albedo factor and average energy of the reflected

gamma rays of iron; **b** Normalized parameters of iron; **c** Saturated gamma number albedo factor and average energy of the reflected gamma rays of lead; **d** Normalized parameters of lead

of 28 cm and lead at a thickness of 10 cm for 1.25 MeV gamma rays. Figure 7a and c shows that the saturation gamma number albedo factors for iron and lead increase with an increase in the gamma incidence angle, and the growth rate also increases.

Figure 7b and d shows the variation in the ratios of saturation gamma number albedo factor, saturation gamma energy albedo factor, and average energy of the saturation reflection gamma, in the case of oblique incidence, divided by the corresponding results for vertical incidence. From the results of these three ratios, compared with the case of vertical incidence, the influence of oblique incidence on the average energy of the saturation reflection gamma is the weakest, corresponding to a factor of two to three, whereas the influence on gamma energy albedo factor is the most significant, a factor greater than five. Compared with iron, the influence of the gamma ray incidence angle on the gamma number albedo factor and average energy albedo factor of lead is more significant owing to the higher atomic number of lead.

### 4 Conclusion

In this study, the Monte Carlo method was used to simulate the gamma albedo factor of single-element materials—iron and lead—as well as multi-element materials—PE and OC—and its influence factors. The relationships between the gamma albedo factor and the effective atomic number of multi-element materials were analyzed. The effective atomic number of materials can be used to characterize the effective nuclear charge number of multi-element materials, which can characterize the interaction between gamma rays and materials and vary with respect to the composition of the material. Comparing the gamma number albedo factor of single-element and multi-element materials, it is clear that the gamma number albedo factor and energy albedo factor of the materials first increase rapidly with an increase in the material thickness; then, both tend to saturate when the thickness of the material reaches a certain value. This conclusion is true not only for single-element materials but also for multi-element materials. Because the intensity of the interaction between gamma rays and materials is related to the incident gamma energy and material type, when the incident

gamma energy is within a certain range, the relative value of the saturation gamma albedo factor depends on the effective atomic number of the materials. When the incident gamma energy is constant and between 0.2 and 2.5 MeV, the saturation gamma number albedo factors and saturation gamma energy albedo factors of lead, iron, OC, and PE increase with a decrease in the effective atomic number. The incident angle of gamma rays also affects the gamma albedo factor. The larger the angle is between the incident direction of the gamma ray and the normal direction of the material surface, the greater the thickness and average energy of the reflected gamma rays under saturation conditions and the saturation gamma number albedo factor are.

**Authors' contributions** All authors contributed to the study conception and design. Material preparation, data collection and analysis were performed by Ying-Hong Zuo, Jin-Hui Zhu and Peng Shang. The first draft of the manuscript was written by Ying-Hong Zuo, and all authors commented on previous versions of the manuscript. All authors read and approved the final manuscript.

## References

1. D. Yılmaz, Z. Uzunoğlu, C. Demir, Albedo factors of some elements in the atomic number range  $26 \leq Z \leq 79$  for 59.54 keV. *Appl. Radiat. Isot.* **122**, 68–71 (2017). <https://doi.org/10.1016/j.apradiso.2017.01.013>
2. S. Azimkhani, F. Zolfagharpour, F. Ziaie, Calculation of thermal neutron albedo for mono-material and bi-material reflectors. *Nucl. Sci. Tech.* **29**, 130 (2018). <https://doi.org/10.1007/s41365-018-0466-1>
3. V.P. Singh, N.M. Badiger, S. Kothan et al., Gamma-ray and neutron shielding efficiency of lead-free gadolinium-based glasses. *Nucl. Sci. Tech.* **27**, 103 (2016). <https://doi.org/10.1007/s41365-016-0099-1>
4. Z. Uzunoğlu, D. Yılmaz, Y. Şahin, Determination of the saturation thickness and albedo factors for mercury(II) oxide and lead(II) oxide. *Instrum. Sci. Technol.* **45**, 111–121 (2016). <https://doi.org/10.1080/10739149.2016.1199032>
5. A.D. Sabharwal, B. Singh, B.S. Sandhu, Investigations of multiple backscattering and albedos of 1.12 MeV gamma photons in elements and alloys. *Nucl. Instr. and Meth. B* **267**, 151–156 (2009). <https://doi.org/10.1016/j.nimb.2008.10.072>
6. A.D. Sabharwal, S. Singh, B. Singh et al., Albedo factors of 279, 320, 511 and 662 keV backscattered gamma photons. *Radiat. Eff. Defects Solids* **166**, 451–458 (2011). <https://doi.org/10.1080/10420150.2010.544039>
7. C.M. Diop, B. Elhamzaoui, J.C. Nimal, Determination of the double angular and energy differential gamma-ray albedo for iron material by using the Monte Carlo method. *Nucl. Sci. Eng.* **117**, 201–226 (1994). <https://doi.org/10.13182/NSE94-A21499>
8. H. Kadotani, A. Shimizu, Gamma ray albedo data generated by the invariant embedding method. *J. Nucl. Sci. Technol.* **35**, 584–594 (1998). <https://doi.org/10.1080/18811248.1998.9733912>
9. M. Biswas, A.K. Sinha, S.C. Roy, Measurement of number albedo of backscattered photons for tin and lead. *J. Nucl. Sci. Technol.* **17**, 559–561 (1980). <https://doi.org/10.3327/jnst.17.559>
10. J. Šeda, J. Kluson, T. Cechák, The calculation of gamma-rays albedo by the MC method. *J. Appl. Radiat. Isot.* **29**, 419–422 (1978). [https://doi.org/10.1016/0020-708X\(78\)90077-7](https://doi.org/10.1016/0020-708X(78)90077-7)
11. B.P. Bulatov, The albedos of various substances for  $\gamma$ -rays from isotropic  $^{60}\text{Co}$ ,  $^{137}\text{Cs}$  and  $^{51}\text{Cr}$  sources. *J. Nucl. Energy, Part A* **13**, 82–84 (1960). [https://doi.org/10.1016/s0368-3265\(60\)80030-8](https://doi.org/10.1016/s0368-3265(60)80030-8)
12. M. Kurudirek, Estimation of effective atomic numbers of some solutions for photon energy absorption in the energy region 0.2–1.5 MeV: an alternative method. *Nucl. Instrum. Methods Phys. Res., Sect. A* **659**, 302 (2011). <https://doi.org/10.1016/j.nima.2011.08.020>
13. M. Kurudirek, Effective atomic numbers, water and tissue equivalence properties of human tissues, tissue equivalents and dosimetric materials for total electron interaction in the energy region 10 keV–1 GeV. *Appl. Radiat. Isot.* **94**, 1 (2014). <https://doi.org/10.1016/j.apradiso.2014.07.002>
14. M. Kurudirek, Effective atomic numbers of different types of materials for proton interaction in the energy region 1 keV–10 GeV. *Nucl. Instrum. Methods Phys. Res., Sect. B* **336**, 130 (2014). <https://doi.org/10.1016/j.nimb.2014.07.008>
15. Y.C. Wu, Multi-functional neutronics calculation methodology and program for nuclear design and radiation safety evaluation. *Fusion Sci. Technol.* **74**, 321–329 (2018). <https://doi.org/10.1080/15361055.2018.1475162>
16. Y.C. Wu, J. Song, H.Q. Zheng et al., CAD-based Monte Carlo program for integrated simulation of nuclear system SuperMC. *Ann. Nucl. Energy* **82**, 161–168 (2015). <https://doi.org/10.1016/j.anucene.2014.08.058>
17. Y.C. Wu, CAD-based interface programs for fusion neutron transport simulation. *Fusion Eng. Des.* **84**, 1987–1992 (2009). <https://doi.org/10.1016/j.fusengdes.2008.12.041>
18. J.H. Hubbell, S.M. Seltzer, Tables of X-Ray mass attenuation coefficients and mass energy-absorption coefficients from 1 keV to 20 MeV for Elements  $Z = 1$  to 92. (1995). <http://www.nist.gov/pml/data/xraycoef/index.cfm>
19. S.S. Obaida, M.I. Sayyedb, D.K. Gaikwada et al., Attenuation coefficients and exposure buildup factor of some rocks for gamma ray shielding applications. *Radiat. Phys. Chem.* **148**, 86–94 (2018). <https://doi.org/10.1016/j.radphyschem.2018.02.026>
20. M.G. Dong, X.X. Xue, V.P. Singh et al., Shielding effectiveness of boron-containing ores in Liaoning province of China against gamma rays and thermal neutrons. *Nucl. Sci. Tech.* **29**, 58 (2018). <https://doi.org/10.1007/s41365-018-0397-x>
21. D.K. Gaikwad, P.P. Pawar, T.P. Selvam, Measurement of attenuation cross-sections of some fatty acids in the energy range 122–1330 keV. *Pramana J. Phys.* **87**, 12 (2016). <https://doi.org/10.1007/s12043-016-1213-y>
22. A.K. Sinha, A. Bhattacharjee, Number albedo measurements from stratified layers of iron, concrete and aluminium. *Pramana* **33**, 493–503 (1989). <https://doi.org/10.1007/BF02846016>
23. V.P. Singh, M.E. Medhat, S.P. Shirmardi, Comparative studies on shielding properties of some steel alloys using Geant4, MCNP, WinXCOM and experimental results. *Radiat. Phys. Chem.* **106**, 255–260 (2015). <https://doi.org/10.1016/j.radphyschem.2014.07.002>
24. A.D. Sabharwal, B. Sandhu, B. Singh, Multiple backscattering on mono-elemental materials and albedo factors of 279, 320, 511 and 662 keV gamma photons. *Phys. Scr.* **83**, 2 (2011). <https://doi.org/10.1088/0031-8949/83/02/025303>